Available online at www.sciencedirect.com

ScienceDirect

Proceedings of the Combustion Institute 36 (2017) 1585–1593

Proceedings of the Combustion Institute

www.elsevier.com/locate/proci

Near limit premixed flamelets in Hele-Shaw cells

Xiaotong Chen [a], Zhanbin Lu [a,*], Shuangfeng Wang [b,c]

[a] *Institute of Applied Mathematics and Mechanics, Shanghai University, Shanghai 200072, China*
[b] *Institute of Mechanics, Chinese Academy of Sciences, Beijing 100190, China*
[c] *School of Engineering Science, University of Chinese Academy of Sciences, Beijing 100049, China*

Received 3 December 2015; accepted 18 August 2016
Available online 13 October 2016

Abstract

In this paper, we report a preliminary attempt to stabilize near limit premixed flamelets in Hele-Shaw cells. As a quasi-two-dimensional analog of flame balls, the flamelet is sustained by diffusive transport alone, with fuel supplied from the open ends of the Hele-Shaw cell, and heat dissipated to the ambient environment through conduction; radiative heat losses from both phases are neglected. Following Spalding's "one-dimensional idealization" approximation, we construct a 2-D model to account for the heat and mass transfer processes in both the gas and the solid phases, with the gap height as a parameter controlling the heat exchange rate between the two phases. For each of the three kinds of wall materials considered, two steady solution branches are obtained as a function of the gap height, one corresponding to large flames and the other to small flames. The large flame branch is critically dependent on the boundary and is therefore of little physical value. Linear stability analysis shows that the small flame branch is unstable to random perturbations. 2-D time dependent numerical simulations indicate that a slightly perturbed steady state on the small flame branch either evolves into a single flamelet drifting to the boundary as a whole, or splits into two drifting to the boundary along opposite directions. A partially open square Hele-Shaw combustor has been proposed and is shown to be able to support stabilized flamelets for a certain range of the degree of opening.

Keywords: Premixed flame; Flame cylinder; Hele-Shaw cell; Near limit; Narrow channel

1. Introduction

Flammability limits of premixed gases and the mechanisms that lead to flame quenching constitute one of the major topics in the study of premixed flames [1]. Near the flammability limit premixed flames may exhibit unique features that are uncommon in premixed flames far from the limit. One example of such uncommon phenomena that are exclusive to near limit mixtures is flame balls, which are spherical premixed flames of vanishing flame speed sustained in quiescent near limit premixtures by diffusive transport alone. The Lewis number of the mixture must be substantially lower than unity, a prerequisite to ensure the development of superadiabatic flame temperature to withstand the excessive heat losses [2].

* Corresponding author. Fax: +86 2136033287.
E-mail addresses: zblu@shu.edu.cn, luzhanbin@gmail.com (Z. Lu).

http://dx.doi.org/10.1016/j.proci.2016.08.059
1540-7489

Zeldovich [3] was the first who pointed out that, in addition to the well-known planar flame front solution, 1-D steady solution of premixed flame combustion can take a spherically symmetrical form, corresponding to a stationary flame ball stabilized in a quiescent mixture. Unfortunately, the adiabatic Zeldovich flame ball solution turned out to be unstable and therefore seemed not to be of much value. It was not until the late 1980s that flame balls began to attract much attention when they were accidentally observed by Ronney in a drop tower experiment [4]. Subsequently, heat losses of various nature, including radiative [5,6], convective [7,8] and conductive [9], have been identified as candidates of mechanisms to account for the observed stable flame balls.

The finding of stabilized flame balls is certainly of great significance to combustion theory, especially to the understanding of flammability limits and chemical kinetics under limiting conditions. However, from the practical perspective, as a unique form of premixed combustion potential applications of flame ball combustion have been rarely explored. The reason may lie in the fact that flame balls can only exist in a microgravity environment, a strict condition that is expensive to achieve on ground-based facilities.

In this paper, we report a preliminary attempt toward the application of flame ball combustion in a Hele-Shaw-type combustor. The inspiration comes from the increasing interests among the combustion community in miniaturized combustors. In the past years, many attempts have been made to explore the possibility of implementing various forms of combustion in micro- or meso-scale combustors. Along this line, it has been found that under certain conditions both premixed and non-premixed flames are possible to be stabilized in narrow tubes or narrow channels [10–14]; see, e.g. the review articles [15–17] for more references. Inspired by these findings, we explore in this work the possibility of stabilizing flame balls in a confined narrow channel, or in other words, a Hele-Shaw cell. This amounts to squeezing a free flame ball from opposite sides by two parallel plates. The squeezed flamelet will take a pie shape in the narrow channel, and therefore thermal interactions between the flame and the channel walls are expected to play a significant role in the stabilization of the premixed flamelet. In this connection, the configuration under consideration is to some extent similar to that described by Shah et al. [18], where the structure and stabilization of flame balls in porous media were explored. However, it should be pointed out that, in their work the heat conductivity of the porous media has been neglected, so that the porous media merely behaves as a heat sink and has no contribution to heat redistribution. By contrast, in the present study, wall thermal conduction behaves as a dominant heat loss mechanism and therefore plays a critical role in the stabilization of the premixed flamelets in Hele-Shaw cells.

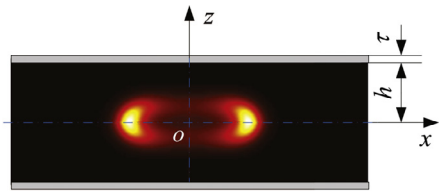

Fig. 1. A schematic diagram showing the cross-sectional view of a premixed flamelet stabilized in a Hele-Shaw cell.

2. Model and formulation

We consider a Hele-Shaw cell consisting of two parallel plates that are separated by a certain distance, as is schematically shown in Fig. 1. Both plates are made of the same material and have the same thickness. The Hele-Shaw cell is initially filled with a near limit fuel-lean combustible mixture, which can support sustained premixed flame combustion through the continual gas supply from the open ends of the Hele-Shaw cell. The chemical reaction taking place in the mixture is modeled by the following single-step irreversible reaction:

$$1\ \text{Fuel} \rightarrow 1\ \text{Products} + \{Q\},$$

implying that one unit mass of fuel is converted into one unit mass of products, releasing an amount Q of energy.

Aiming at a qualitative understanding of the problem, we employ the constant density model to describe the combustion processes taking place in the gaseous phase, and assume that all the involved physicochemical parameters take constant values. The outer surfaces of the two plates are assumed to be perfectly insulated such that the only origin of heat losses of the system comes from the boundaries of the Hele-Shaw cell, where the temperatures of the gaseous and solid phases are assumed to be equal to that of the ambient and the fuel mass fraction is kept at the constant supply value. Furthermore, the thickness of the plates is assumed to be so small that the wall temperature can be regarded as uniform along the normal direction. Consequently, if length is scaled by $D_{\text{th}}/S_{\text{L}}$, where D_{th} is the gas phase thermal diffusivity and S_{L} is the laminar flame speed corresponding to the ambient fuel mass fraction Y_{f}, time is scaled by $D_{\text{th}}/S_{\text{L}}^2$, fuel mass fraction is scaled by Y_{f}, and temperature is scaled by $T_{\text{b}} - T_{\text{f}} = QY_{\text{f}}/c_p$ where T_{b} and T_{f} are the adiabatic flame temperature and the ambient temperature, respectively, and c_p is the specific heat (at constant pressure) of the gaseous phase, then in the coordinate system shown in Fig. 1 the governing

equations describing the system can be expressed in dimensionless form as:

$$\begin{aligned}\frac{\partial\theta}{\partial t} &= \nabla^2\theta + \Omega,\\ \frac{\partial Y}{\partial t} &= \frac{1}{\mathrm{Le}}\nabla^2 Y - \Omega,\\ \frac{1}{r_{_D}}\frac{\partial\theta_{\mathrm{w}}}{\partial t} &= \nabla_{\perp}^2\theta_{\mathrm{w}} \mp \frac{1}{\tau r_{_\lambda}}\left.\frac{\partial\theta}{\partial z}\right|_{z=\pm h},\end{aligned} \tag{1}$$

corresponding to energy balance of the gaseous phase, mass balance of the fuel, and energy balance of the wall, respectively. Here in Eq. (1), $\theta = (T - T_{\mathrm{f}})/(T_{\mathrm{b}} - T_{\mathrm{f}})$ and $\theta_{\mathrm{w}} = (T_{\mathrm{w}} - T_{\mathrm{f}})/(T_{\mathrm{b}} - T_{\mathrm{f}})$ stand for, respectively, the dimensionless temperature of the gaseous phase and the dimensionless wall temperature, Y stands for the normalized fuel mass fraction, $r_{_\lambda} = \lambda_{\mathrm{w}}/\lambda$ and $r_{_D} = D_{\mathrm{w}}/D_{\mathrm{th}}$ represent, respectively, the ratios of heat conductivities and thermal diffusivities between the solid and gaseous phases, $\mathrm{Le} = D_{\mathrm{th}}/D$ is the Lewis number with D denoting the fuel mass diffusivity, and h and τ are, respectively, the dimensionless half separation distance between the two plates and the dimensionless plate thickness. In the wall energy balance equation, $\nabla_{\perp}^2 = \partial^2/\partial x^2 + \partial^2/\partial y^2$ represents the Laplacian on the xy plane, and the last term on the r.h.s. describes the heat exchange between the gas and the wall due to the vertical gas temperature gradient. An Arrhenius type kinetics is assumed for the chemical reaction so that the dimensionless reaction rate Ω takes the form

$$\Omega = \frac{\beta^2}{2\,\mathrm{Le}}\, Y \exp\left\{\frac{\beta(\theta-1)}{(1+q\theta)/(1+q)}\right\}, \tag{2}$$

where $\beta = E(T_{\mathrm{b}} - T_{\mathrm{f}})/RT_{\mathrm{b}}^2$ is the Zeldovich number, with E and R the activation energy and the universal gas constant, respectively, and $q = (T_{\mathrm{b}} - T_{\mathrm{f}})/T_{\mathrm{f}}$ denotes the thermal expansion parameter.

The Hele-Shaw system under consideration is symmetrical with respect to $z = 0$ and is maintained at the ambient condition at the inlets, so the dimensionless boundary conditions satisfied by Eq. (1) can be written as

$$\begin{aligned}&\underline{\text{at the inlets}}, && \theta = 0, && Y = 1, && \theta_{\mathrm{w}} = 0,\\ &\underline{\text{at } z = 0}, && \frac{\partial\theta}{\partial z} = 0, && \frac{\partial Y}{\partial z} = 0,\\ &\underline{\text{at } z = \pm h}, && \theta = \theta_{\mathrm{w}}, && \frac{\partial Y}{\partial z} = 0.\end{aligned} \tag{3}$$

The 3-D gas phase conservation equations formulated in Eq. (1) may be further simplified by taking advantage of the narrow character of the Hele-Shaw cell. Similar to Spalding's "one-dimensional idealization" treatment for premixed flames in narrow ducts [1], an average of θ and Y over the z direction may be taken as a representation of the gas temperature and fuel mass fraction distributions on the xy plane, while the gas temperature gradients at the walls are determined by a linear approximation of the vertical temperature profiles. Specifically, under linear approximation the average temperature $\bar{\theta} = \theta_{\mathrm{w}} - (h/2)\,\partial\theta/\partial z|_{z=h}$, so the wall temperature gradient can be approximated by $\partial\theta/\partial z|_{z=h} = 2(\theta_{\mathrm{w}} - \bar{\theta})/h$. Consequently, Eq. (1) is simplified to the following 2-D form:

$$\begin{aligned}\frac{\partial\theta}{\partial t} &= \nabla_{\perp}^2\theta + \Omega - \frac{2}{h^2}(\theta - \theta_{\mathrm{w}}),\\ \frac{\partial Y}{\partial t} &= \frac{1}{\mathrm{Le}}\nabla_{\perp}^2 Y - \Omega,\\ \frac{1}{r_{_D}}\frac{\partial\theta_{\mathrm{w}}}{\partial t} &= \nabla_{\perp}^2\theta_{\mathrm{w}} + \frac{2}{h\tau r_{_\lambda}}(\theta - \theta_{\mathrm{w}}),\end{aligned} \tag{4}$$

where for conciseness the overline symbols in $\bar{\theta}$ and $\overline{Y}$ have been omitted.

Equation (4) and the inlet conditions presented in (3) define the mathematical problem to be studied in this paper. There are totally 7 dimensionless parameters involved in the problem, namely Le, β and q, characterizing properties related to the gaseous phase, $r_{_\lambda}$, $r_{_D}$ and τ, characterizing properties related to the wall material, and the half gap height h, which serves as the primary parameter controlling the heat exchange rate between the gas and solid phases.

3. 1-D steady solutions

In this Section, we examine 1-D steady solutions of Eq. (4), corresponding to axisymmetric flame cylinders established in circular Hele-Shaw cells. The spatial derivatives involved in the 1-D steady form of Eq. (4) were discretized by a fourth-order central difference scheme, then the resulting system of nonlinear algebraic equations was solved by using a continuation method, which consists of an Euler predictor step and a Newton corrector step [19]. One of the merits of the continuation method is that it can capture all the possible solutions on multiple solution branches, whether stable or not. Three typical wall materials are considered, namely quartz glass, stainless steel and aluminum, whose thermophysical parameter values are given in Table 1. Throughout this work we choose $\mathrm{Le} = 0.3$, $\beta = 8$, $q = 1$, corresponding to typical near limit light fuel flames. For all materials considered the thickness of the wall is fixed at $\tau = 1$, so for a specified wall material the only control parameter is the half gap height h.

Before presenting the steady solutions it is worth pointing out that a significant difference exists between flame cylinders and flame balls in connection with their structural characteristics. Recall that under spherical symmetry both θ and Y vary as r^{-1} in the far field so the conservation equations admit a 1-D adiabatic steady solution in an infinite space, corresponding to the classical Zeldovich flame ball

Table 1
Material thermophysical parameter values.

Material	Density (g/cm^3)	Heat conductivity (J/cm/s/K)	Specific heat (J/g/K)
Gas mixture	1.0×10^{-3}	4.0×10^{-4}	1.1
Quartz glass	2.2	1.4×10^{-2}	0.8
Stainless steel	8.0	0.162	0.5
Aluminum	2.7	2.2	0.9

solution with a finite radius R_Z [3]. By contrast, in cylindrical geometry θ and Y vary as $\ln r$ in the far field, thereby negating the existence of a 1-D adiabatic steady flame cylinder solution in an infinite space. In a study addressing the peristaltic instability of flame cylinders, Buckmaster [20] bypassed the far field logarithmic singularity of flame cylinders by assuming a prescribed flame cylinder radius $\bar{R}$ in the analysis, which was equivalent to choosing a finite domain boundary $\bar{r}_B = \bar{R} \cdot e^{1/\bar{R}}$, where $\bar{r}_B$ and $\bar{R}$ are made dimensionless by the Zeldovich radius R_Z. The stability analysis results thus obtained successfully accounted for the g-jitter effects of flame balls observed in reduced-gravity experiments on board parabolic flights. In the present study we follow Buckmaster's treatment by considering flamelets developed in Hele-Shaw cells of finite dimensions. The results herein presented may be quantitatively dependent on the choice of the cell size, yet it is believed that the qualitative features revealed will not be significantly influenced by such choices.

Typical 1-D steady solutions corresponding to the above-mentioned three wall materials are illustrated in Fig. 2 (note the log scale for the r-axis), where the Hele-Shaw cell radius is chosen to be $r_B = 50$ and the half gap height is kept at $h = 3.5$. It is evident that, for each wall material the gas temperature around the flame cylinder is considerably larger than that of the wall, such that besides the heat lost to the boundary through gas phase heat conduction, there is a substantial portion of heat transferred from the flame to the wall, and is eventually dissipated to the boundary through solid heat conduction. When the cell boundary is approached, however, the gas and wall temperature profiles tend to collapse and hence heat transfer between the two phases ceases. These observations indicate that, for the currently considered Hele-Shaw configuration, heat transfer between the gas and solid phases is always one-way, that is, from the gas to the solid; there is no recirculation of heat from the wall to the gas by preheating. Figure 2 also shows that increasing the wall heat conductivity tends to reduce the slope of the wall temperature profile, and as a result of the enhancement of heat loss toward the wall, the flame cylinder shrinks and the flame temperature rises.

The dependence of the flame cylinder radius on h for the three wall materials is illustrated in Fig. 3, where the flame cylinder radius R is identified with the location that achieves the maximum reaction rate. As can be seen, for each wall material there exist two solution branches when h is smaller than a critical value h_{max}, one corresponding to small flame cylinders while the other corresponding to large ones. Figure 4 shows the 1-D responses of flame cylinders in steel Hele-Shaw cells with three different plate radii. It indicates that the large flame branch is critically dependent on the location of the boundary and is therefore of little physical value; by contrast, the small flame branch is not quite sensitive to the change of r_B and hence constitutes the main focus of the present study. For a specific wall material and a given plate radius, on the small flame branch the flame cylinder radius decreases with decreasing h until a minimum half gap height h_{ext} is reached, where the flame is quenched due to excessive heat loss to the wall. Results indicate that the extinction half gap height h_{ext} increases slightly with the wall heat conductivity, changing from $\approx$ 1.9 for glass to $\approx$ 2.2 for aluminum. The opposite extinction limit h_{max} is apparently due to the 1-D idealization approximation, which is no longer valid when the gap height becomes too large. To explore the flame behavior under such conditions, the complete 3-D Eqs. (1) and (3) must be resorted to instead.

4. Linear stability analysis

We examine the linear stability of the above 1-D steady solutions by numerical normal mode analysis methods. To this end, an infinitesimal perturbation is introduced to the 1-D steady solution such that the perturbed solution takes the form

$$(\theta, Y, \theta_w) = (\theta^*, Y^*, \theta_w^*) + \varepsilon(\theta', Y', \theta_w')e^{\sigma t + im\phi}, \tag{5}$$

where m is the perturbation wave number, σ is the growth rate, and ε is an infinitesimally small parameter characterizing the amplitude of the perturbation. The variables with superscript * denote the 1-D steady solution, whereas those with superscript $'$ denote the radial distribution of the perturbation. Substituting Eq. (5) into(4) and discarding the higher order terms yields the following

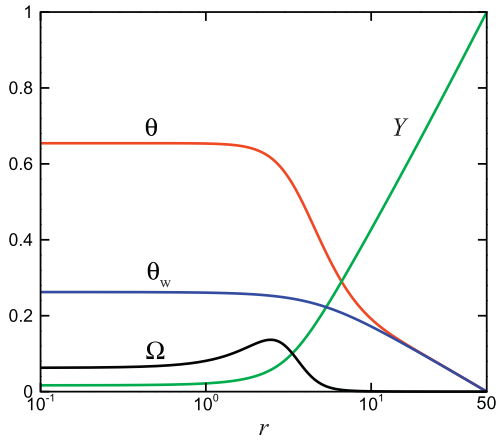

(a) Glass

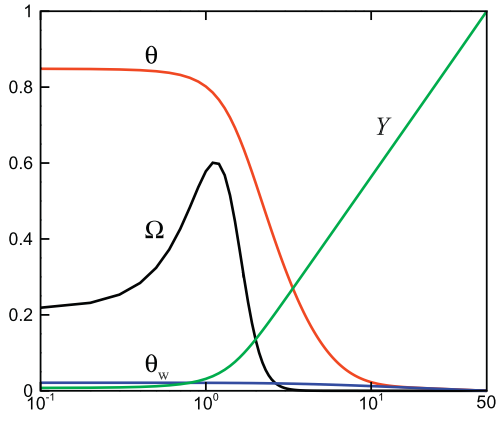

(b) Steel

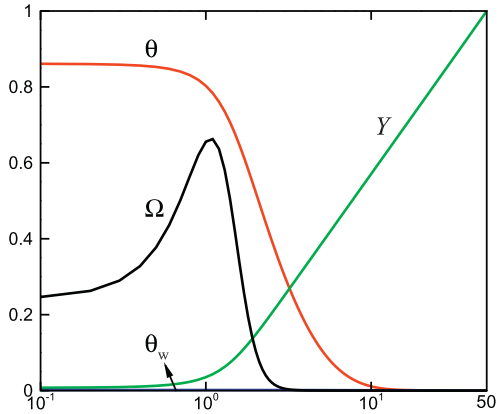

(c) Aluminum

Fig. 2. Typical 1-D axisymmetric steady solutions for flame cylinders established in circular Hele-Shaw cells of different wall materials. The Hele-Shaw cell radius $r_B = 50$ and the half gap height $h = 3.5$ for all the three cases.

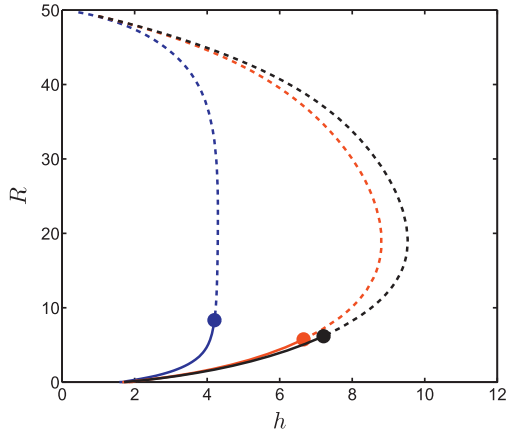

Fig. 3. Response curves showing the dependence of the flame cylinder radius R on the half gap height h for the three wall materials. The curves correspond, from left to right, to glass, steel and aluminum walls, respectively. Solid and dashed lines correspond, respectively, to solutions that are stable and unstable to radial perturbations ($m = 0$); filled circles mark the marginal stability points. Hele-Shaw cell radius $r_B = 50$.

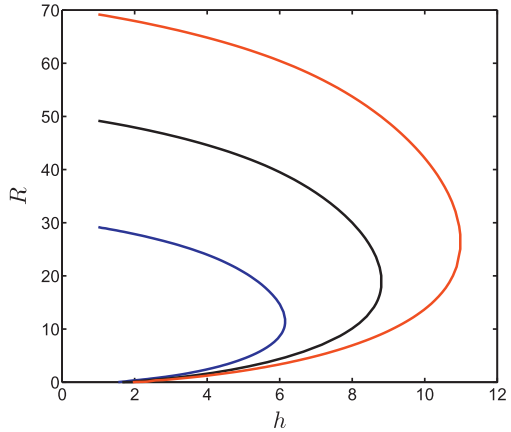

Fig. 4. Response curves showing the dependence of the flame cylinder radius R on the half gap height h for steel Hele-Shaw cells. The curves correspond, from left to right, to plate radius $r_B = 30$, 50 and 70, respectively.

perturbation equations for θ', Y' and θ'_w:

$$0 = \frac{d^2\theta'}{dr^2} + \frac{1}{r}\frac{d\theta'}{dr} - \left(\sigma + \frac{2}{h^2} + \frac{m^2}{r^2}\right)\theta' + \frac{2}{h^2}\theta'_w + \Omega',$$

$$0 = \frac{1}{\mathrm{Le}}\left(\frac{d^2Y'}{dr^2} + \frac{1}{r}\frac{dY'}{dr}\right) - \left(\sigma + \frac{1}{\mathrm{Le}}\frac{m^2}{r^2}\right)Y' - \Omega',$$

$$0 = \frac{d^2\theta'_w}{dr^2} + \frac{1}{r}\frac{d\theta'_w}{dr} - \left(\frac{\sigma}{r_D} + \frac{2}{h\tau r_\lambda} + \frac{m^2}{r^2}\right)\theta'_w + \frac{2}{h\tau r_\lambda}\theta', \tag{6}$$

where

$$\Omega' = \Omega^* \left[\frac{Y'}{Y^*} + \beta\theta' \left(\frac{1+q}{1+q\theta^*} \right)^2 \right], \tag{7}$$

with Ω^* denoting the reaction rate corresponding to the 1-D steady solution.

All perturbations must vanish at the inlet so the boundary conditions there are:

$$\text{at } r = r_B, \quad \theta' = 0, \quad Y' = 0, \quad \theta'_w = 0. \tag{8}$$

The boundary conditions at $r = 0$ are contingent on the perturbation wave number m. If only radial perturbation is present, that is $m = 0$, the symmetrical condition at the center requires

$$\text{at } r = 0, \quad \frac{d\theta'}{dr} = 0, \quad \frac{dY'}{dr} = 0, \quad \frac{d\theta'_w}{dr} = 0. \tag{9}$$

For $m > 0$, the uniqueness condition at the center requires

$$\text{at } r = 0, \quad \theta' = 0, \quad Y' = 0, \quad \theta'_w = 0. \tag{10}$$

Upon discretization by a second-order finite difference scheme, the system of ordinary differential equations (6) with boundary conditions (8–10) is transformed to a matrix eigenvalue problem of the form $\mathbf{A} \cdot \mathbf{x} = \sigma \cdot \mathbf{x}$, which can be solved numerically by standard eigenpackages. For each 1-D steady solution a dispersion relation can be obtained, characterized by the growth rate σ as a function of the discrete perturbation wave number m. Negative and positive growth rates correspond, respectively, to stable and unstable states under the considered perturbation wave number. Figure 3 illustrates the stability analysis results for the 1-D steady solutions with the three wall materials under radial perturbations ($m = 0$). It is evident that for each wall material, the entire large flame branch and a portion of the small flame branch are unstable to radial perturbations. However, with the decrease of h radial stability is achieved for the rest portion of the small flame branch.

2-D stability of the steady solutions is exemplified by the stability diagram shown in Fig. 5, where the marginal stability boundary for $m \geq 1$ is delineated for the small flame branch of the steel plate case. It is evident that the entire small flame branch is unstable to perturbations with wave number $m = 1$. Then, with the increase of m the marginal stability boundary shifts rapidly to the right, until reaching the right extinction boundary h_{max} at $m = 8$. Hence, the entire small flame branch is stable when subjected to azimuthal perturbations with $m \geq 8$, but is unstable for at least one wave number over the range $0 \leq m < 8$. Similar results have been obtained for the quartz glass and aluminum plate cases, so we are led to the conclusion that practically no flame cylinders can be stabilized in the currently considered fully open Hele-Shaw cell configuration, at least for the three kinds of plate materials under consideration.

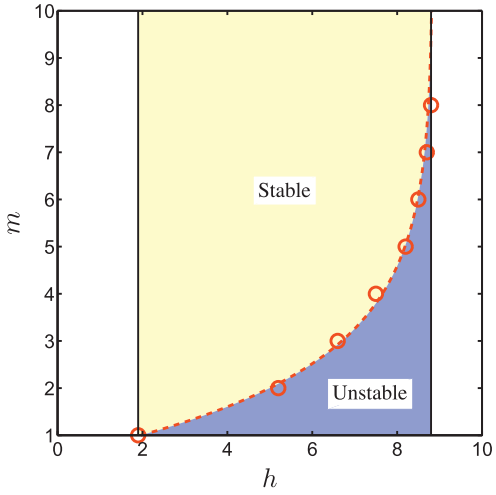

Fig. 5. A stability diagram characterizing the azimuthal stability of the steady solutions on the small flame branch of the steel plate case. The left and right extinction boundaries are, respectively, $h_{ext} \approx 1.9$ and $h_{max} \approx 8.8$.

5. 2-D numerical simulations

2-D numerical simulations have been performed to examine how the steady flame cylinder solutions evolve in Hele-Shaw cells after the onset of instability. A square computational domain with side length $L = 100$ has been employed. A rectangular coordinate system with origin at the center was adopted and the computational domain was discretized using a mesh that is uniform in both the x and y directions. For those grid points outside or on the circle with a radius $r_B = 50$ the inlet conditions in (3) were applied throughout the calculations. This is equivalent to approximating the continuous circular domain boundary by a series of discrete grid points distributed along the periphery of the circle. Time dependent calculations of the unsteady Eqs. (4) were carried out, with the spatial derivatives approximated by a fourth-order central difference scheme, and the time derivatives by an explicit first-order Euler scheme. Initial conditions were taken as the axisymmetric steady solutions perturbed by a random noise upon the gas temperature field.

Figure 6 displays the subsequent development of a randomly perturbed flame cylinder in a circular steel plate Hele-Shaw cell, represented by reaction rate contours at four time instants (note in each graph only a square portion of the computational domain is illustrated to show the details of the flame). The half gap height of the Hele-Shaw cell is $h = 5.0$ which, according to the linear stability analysis results shown in Figs. 3 and 5, corresponds to a steady solution that is stable to perturbations with all the wave numbers except $m = 1$. As

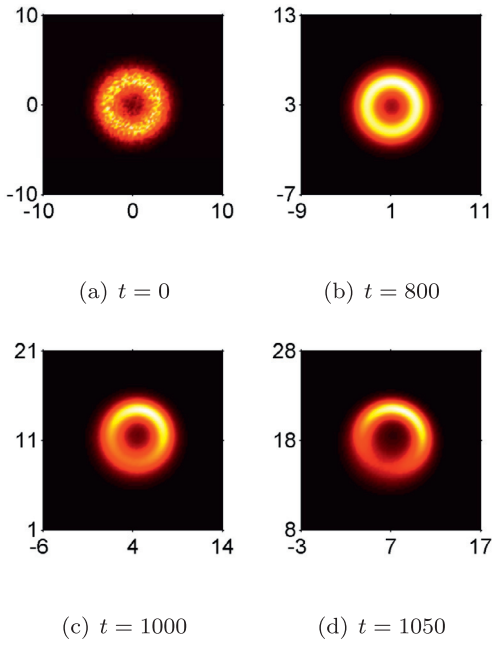

Fig. 6. Reaction rate contours showing the development of a slightly perturbed flame cylinder in a circular steel Hele-Shaw cell with radius $r_B = 50$ and half gap height $h = 5.0$. Horizontal axis: x; vertical axis: y.

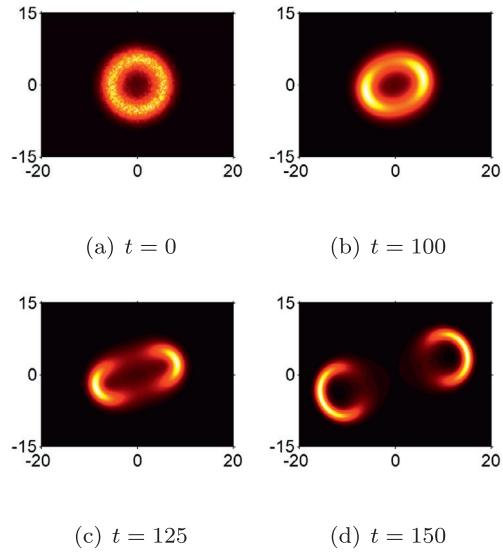

Fig. 7. Reaction rate contours showing the development of a slightly perturbed flame cylinder in a circular steel Hele-Shaw cell with radius $r_B = 50$ and half gap height $h = 6.5$. Horizontal axis: x; vertical axis: y.

can be seen, after an initial transient, the cylindrical symmetry of the flame cylinder is gradually broken, resulting in a polarized circular flamelet that drifts toward the cell boundary. It is found that the reaction rate at the head part of the flamelet is continuously intensified during this process and hence the drift is accelerating with the approach of the boundary.

Time evolution of a perturbed flame cylinder in a circular steel Hele-Shaw cell with $h = 6.5$ is shown in Fig. 7. The corresponding steady solution is unstable to perturbations with two wave numbers, $m = 1$ and $m = 2$, the latter having a larger growth rate. As is shown, the flame cylinder eventually splits into two flamelets, which then drift toward the boundary along opposite directions.

The mechanism underlying the drifting flame cylinders may be accounted for by the competition between two counteracting factors, that is, heat loss toward the ambient and fuel intake from the boundary. The flame cylinder consumes fuel that is fed from the boundary, generating heat that eventually dissipates back to the ambient through the boundary. The closer the flame cylinder is to the boundary, the steeper the temperature gradients in both the gas and solid phases, and thus the larger the amount of heat lost to the boundary. At the same time, however, due to the increase of the fuel mass fraction gradient, fuel supplying to the flame cylinder is also enhanced with the approach of the flame cylinder to the boundary. The sub-unity Lewis number presently considered implies that fuel mass diffusion outperforms heat dissipation and therefore the flame cylinder is expected to drift toward the boundary.

According to the above analysis of the drifting mechanism, possible measures that may be taken to stabilize the flame cylinders in Hele-Shaw cells are either to enhance the heat loss or to reduce the fuel supply at the cell inlets. We propose here a method that essentially follows the second line. As schematically shown in Fig. 8, we choose a square Hele-Shaw cell, on each side of which the boundary is partially sealed in the middle, such that only the four corners of the Hele-Shaw cell are open to the ambient atmosphere. Each corner is characterized by an opening width l on each side and the local fuel mass fraction at the opening mouth is still fixed at $Y = 1$. On all the boundaries the gas and wall temperatures are kept equal to that of the ambient, that is, $\theta = \theta_w = 0$. As a result, compared with the previous fully open cell case, the heat loss for the current partially open cell remains essentially unchanged but the fuel supply is significantly reduced. Time dependent calculations were carried out for a flame cylinder in such a partially open steel Hele-Shaw cell, which has a half gap height $h = 6.5$, side length $L = 100$ and opening width $l = 15$ at each of the four corners. The corresponding perturbed axisymmetric steady solution with the same gap height was adapted to the square domain as the initial condition. The calculation results indicate that the initial perturbations are damped out and the steady

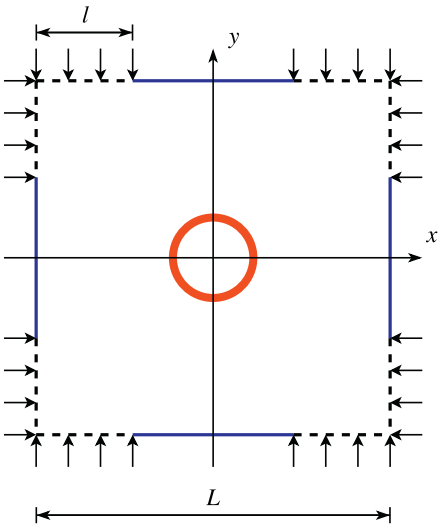

Fig. 8. A schematic diagram showing a partially open square Hele-Shaw cell.

state flame cylinder is restored, as is illustrated in Fig. 9 by the contour plots. Further calculations with varying l indicated that stabilized flamelets can be supported by such partially open square Hele-Shaw combustors over a certain range of the degree of opening.

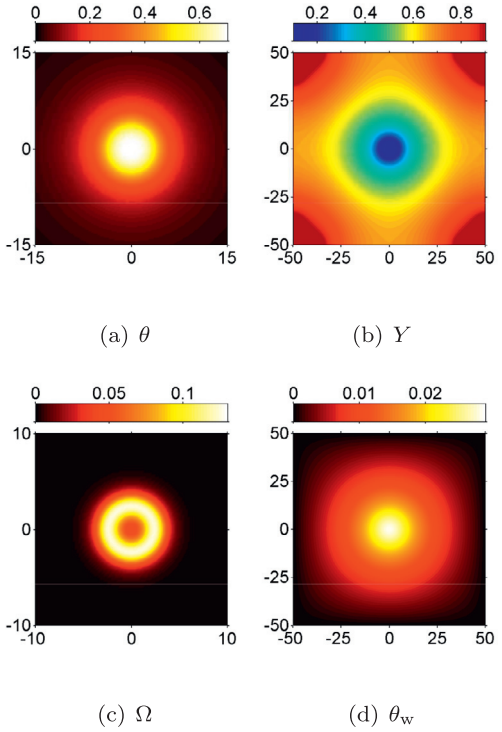

Fig. 9. Contour plots showing the eventual steady state of a slightly perturbed flame cylinder in a partially open square steel Hele-Shaw cell with side length $L = 100$ and half gap height $h = 6.5$. The opening width $l = 15$ on each side of the cell. Horizontal axis: x; vertical axis: y.

6. Conclusions and discussions

Near limit premixed flame combustion in Hele-Shaw cells was studied within the framework of a constant density model by using numerical approaches. A low Lewis number fuel-lean mixture was considered, such that near the inflammability limit a stationary circular premixed flamelet may stabilize in the Hele-Shaw cell, as a quasi-two-dimensional analog of the well-known stationary flame ball solution in an unconfined quiescent fuel-lean mixture. By exploiting the narrowness of the Hele-Shaw cell, an approximation in the spirit of Spalding's "one-dimensional idealization" has been introduced to describe the gas phase combustion field. As a result, the problem becomes equivalent to one that has a two-dimensional flame cylinder confined in a narrow channel, with the channel half height h as the control parameter that determines the heat exchange rate between the gas and the channel wall.

For each channel wall material considered, with the variation of h two axisymmetric steady solution branches were identified, one corresponding to large flame cylinders and the other to small flame cylinders. Linear stability analysis showed that the steady solutions on both branches are unstable to random perturbations, thereby eliminating the possibility of stabilized flame cylinders in fully open Hele-Shaw cells. 2-D time dependent numerical simulations indicated that the slightly perturbed steady states either evolve into a curved flame front drifting to the boundary, or split into two flame fronts that drift to the boundary along opposite directions. A partially open square Hele-Shaw combustor has been proposed, and was shown to be able to support stabilized flame cylinders for a certain range of the degree of opening.

As a preliminary attempt, the present study accounts only for conductive heat losses through the Hele-Shaw cell boundaries and neglects radiative heat losses from both the gaseous and solid phases. Taking these radiative heat losses into account is not likely to alter the physical picture in a qualitative manner, as the experience from flame ball research confirms that different types of heat losses play a similar role in the stabilization of flame balls. Another approximation made in the present study, the "one-dimensional idealization", is expected to underestimate the maximum temperature and the flame radius, especially when the channel height becomes too large. However, we believe that such an approximation is adequate for the purpose of

capturing the essential structural and stabilization characteristics of near limit premixed flamelets in Hele-Shaw cells. Hence, qualitative comparisons may be made between the current numerical predictions and carefully designed experiments.

Acknowledgments

This work was supported by the National Science Foundation of China, under grant nos. 50706024 and 11472167, and the Shanghai Rising Star Program, under grant no. 09QA1402300. The work of S.F. Wang was supported by the Strategic Pioneer Program on Space Science, Chinese Academy of Sciences, grant no. XDA04020410.

References

[1] D.B. Spalding, *Proc. R. Soc. Lond. A* 240 (1957) 83–100.
[2] C. Lee, J. Buckmaster, *SIAM J. Appl. Math.* 51 (5) (1991) 1315–1326.
[3] Ya. B. Zeldovich, Theory of Combustion and Detonation of Gases, Academy of Sciences (USSR), Moscow, 1944.
[4] P. Ronney, *Combust. Flame* 82 (1990) 1–14.
[5] J. Buckmaster, G. Joulin, P. Ronney, *Combust. Flame* 79 (1990) 381–392.
[6] J. Buckmaster, G. Joulin, P. Ronney, *Combust. Flame* 84 (1991) 411–422.
[7] J. Buckmaster, G. Joulin, *J. Fluid Mech.* 227 (1991) 407–427.
[8] G. Joulin, P. Cambray, N. Jaouen, *Combust. Theory Model.* 6 (2002) 53–78.
[9] J. Buckmaster, G. Joulin, *Combust. Sci. Tech.* 89 (1993) 57–69.
[10] F. Richecoeur, D. Kyritsis, *Proc. Combust. Inst.* 30 (2005) 2419–2427.
[11] K. Maruta, T. Kataoka, N. Kim, S. Minaev, R. Fursenko, *Proc. Combust. Inst.* 30 (2005) 2429–2436.
[12] T. Jackson, J. Buckmaster, Z. Lu, D. Kyritsis, L. Massa, *Proc. Combust. Inst.* 31 (2007) 955–962.
[13] J. Bieri, V. Kurdyumov, M. Matalon, *Proc. Combust. Inst.* 33 (2011) 1227–1234.
[14] J. Wan, A. Fan, K. Maruta, H. Yao, W. Liu, *Int. J. Hydrog. Energy* 37 (24) (2012) 19190–19197.
[15] A. Fernandez-Pello, *Proc. Combust. Inst.* 29 (2002) 883–899.
[16] K. Maruta, *Proc. Combust. Inst.* 33 (2011) 125–150.
[17] Y. Ju, K. Maruta, *Prog. Energy Combust. Sci.* 37 (6) (2011) 669–715.
[18] A. Shah, R. Thatcher, J. Dold, *Combust. Theory Model.* 4 (2000) 511–534.
[19] W.C. Rheinboldt, *SIAM J. Num. Anal.* 17 (1980) 221–237.
[20] J. Buckmaster, *Combust. Sci. Tech.* 84 (1992) 163–176.